Proceedings of the Second IASTED Africa Conference
Power and Energy Systems (AfricaPES 2008)
September 8-10, 2008 Gaborone, Botswana

DYNAMIC MODEL AND CONTROL OF POWER CONVERTERS FOR GRID CONNECTED RENEWABLE ENERGY SYSTEMS

A.F Nnachi, D.V Nicolae, *member IEEE* and A.A Jimoh, *member IEEE*
Department of Electrical and Electronics Engineering
Tshwane University of Technology
P.O.Box X680, Pretoria 0001, South Africa
nnachiaf@tut.ac.za, NicolaeDV@tut.ac.za, jimohaa@tut.ac.za

ABSTRACT

In order to investigate certain dynamic events of a grid connected renewable energy system (RES), a systematic model and control is developed. The RES with its converter is taken as a controlled dc current source and the grid side converter model is based on approximate power balance of the dc-link and the ac-side. Here an AC-side decoupled current controller in dq reference frame and simplified net dc-bus voltage controllers are implied.

Among different dynamic events that is studied, the response of the system during three-phase to ground fault, step change in reference DC voltage, active and reactive power change are studied and presented.

KEY WORDS

Converter, dynamic model, controller, Renewable energy.

1. Introduction

In recent years, the global electrical energy consumption is steadily rising and there is therefore continuous demand to increase the power generation capacity. A significant percentage of the required capacity increase can be based on renewable energy sources or distributed generation systems. Systems such as Wind turbine, micro turbines, photovoltaic and fuel cell systems will be serious contributors to the power supply.

Grid connection of renewable energy systems will allow the consumer to feed its own load utilizing the available energy, and the surplus energy can be injected into the grid under the energy buy-back scheme to reduce the payback period. When this RES is integrated with the utility grid, a two-way power flow is established [1], [2].

Continuous advances in high power semiconductor devices have made voltage source converter (VSC) a technically viable, efficient and important interface to the grid for the renewable. This paper therefore presents a dynamic model and control of grid connected renewable via a neutral point converter (NPC) VSC.

A small signal dynamic model of the grid connected renewable energy systems is developed. The analysis and control scheme which is done in a dq reference frame is intended to achieve constant dc-link, obtain unity power factor and allow bi-directional power flow. Dynamic response of the system during three-phase to ground fault, step change in reference DC voltage, active and reactive power change are studied and presented.

2. Mathematical Model

Fig. 1 shows a schematic diagram of a grid connected renewable system via a NPC. The system is made of a grid connected three-level NPC and a RES connected power electronics converter linked by DC-bus. The Resistor R_{DC} represents the total switching loss of inverter or it could represent the DC load in case the converter operates as a rectifier. It is assumed that the DC-bus capacitors are equal. P_{in} represents the power flow between the RES side converter and the grid side converter and is used as a basis to develop the overall system model. R is internal resistance of the smoothing inductor L [3]. The emphases here is the modeling of the grid side converter hence the RES is modeled as a controlled current source.

The technique of modeling a converter as a rectifier or as an inverter is the same; the only difference is the definition of power sign. Modeling the grid side inverter, the inverter output voltage (V_{ta}, V_{tb}, V_{tc}), the grid voltage (V_{sa}, V_{sb}, V_{sc}) and the AC neutral point voltage V_{no} can be related by the state space equation

$$\frac{d}{dt}[i_{abc}] = [A][i_{abc}] + [B][V_{abcn}] + [C]V_{no} \tag{1}$$

where $[i_{abc}] = [i_a \; i_b \; i_c]^T$

$$A = \begin{bmatrix} -R/L & 0 & 0 \\ 0 & -R/L & \\ 0 & & 0 - R/L \end{bmatrix} \quad B = \begin{bmatrix} -1/L & 0 & 0 \\ 0 & -1/L & \\ 0 & & 0 - 1/L \end{bmatrix} \quad [V_{abcn}] = \begin{bmatrix} V_{sa} - V_{tan} \\ V_{sa} - V_{tan} \\ V_{sa} - V_{tan} \end{bmatrix}$$

$$[C] = [-1/L \;\; -1/L \;\; -1/L]^T$$

This equation (1) represents the discrete time-variant large signal model of the inverter.

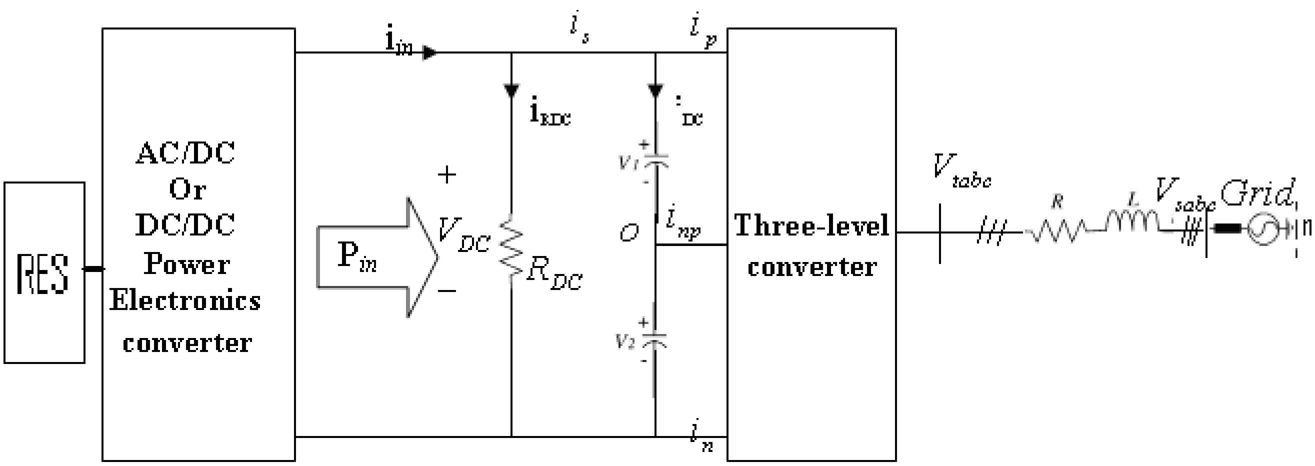

Figure 1. Grid connected RES via three-level NPC converter

Transforming equation (1) into rotating *dqo* frame based on the transformation $\lfloor f_{dqo} \rfloor = T_{dq0}(\omega t)[fabc]$ [4] where

$$T_{dq0} = \frac{2}{3}\begin{bmatrix} \cos\omega t & \cos\left(\omega t - \frac{2\pi}{3}\right) & \cos\left(\omega t + \frac{2\pi}{3}\right) \\ \sin\omega t & \cos\left(\omega t - \frac{2\pi}{3}\right) & \cos\left(\omega t - \frac{2\pi}{3}\right) \\ 1/\sqrt{2} & 1/\sqrt{2} & 1/\sqrt{2} \end{bmatrix} \tag{2}$$

$$\frac{d}{dt}[i_{dqo}] = [A][i_{dqo}] + [B][V_{dqon}] + [C]V_{no} \tag{3}$$

where

$$[i_{dqo}] = [i_d\ i_q\ i_0]^T, \quad [V_{dqon}] = \begin{bmatrix} V_{sd} - V_{td} \\ V_{sq} - V_{tq} \\ V_{so} - V_{to} \end{bmatrix} [C] = \left[0\ 0\ -\sqrt{3}/L\right]^T$$

where ω is the line angular frequency. As the sum of the three line currents is zero, there is no homo-polar component ($I_0 = 0$). Therefore the AC NP voltage V_{no} does not affect any transformed current.

Substituting $I_0 = 0$ into the homo-polar component of the equation (3),

$$\frac{dI_o}{dt} = \left[-R/L\right] I_o - 1/L[V_{so} - V_{to}] + \left[-\sqrt{3}/L\right]V_{no}$$
$$0 = 0 - 1/L[V_{so} - V_{to}] + \left[-\sqrt{3}/L\right]V_{no}; \quad V_{no} = \frac{[V_{so} - V_{to}]}{\sqrt{3}} \tag{4}$$

When the electrical grid is balanced, the average value of V_{so} is zero, hence V_{no} depends only on the homo-polar component of the AC voltages of the converter

Moreover the rotating reference frame is synchronized and aligned with the grid in such a way that $V_{sq} = 0$, substituting this and omitting the homopolar component equation (5) becomes

$$\frac{d}{dt}\begin{bmatrix} I_d \\ I_q \end{bmatrix} = \begin{bmatrix} -R/L & \omega \\ -\omega & -R/L \end{bmatrix}\begin{bmatrix} I_d \\ I_q \end{bmatrix} + \begin{bmatrix} -1/L & 0 \\ 0 & -1/L \end{bmatrix}\begin{bmatrix} V_{td} \\ V_{tq} \end{bmatrix} + \begin{bmatrix} -1/L \\ 0 \end{bmatrix} V_{sd} \tag{5}$$

3. The DC Side of the System

Taking into account that the dq transformation is power conservative, the instantaneous power at the DC side can be related to the AC side. In doing this, the switching function can be avoided. The active and reactive power of a three-phase system is given by

$$P_{AC} = \frac{3}{2}(V_d I_d + V_q I_q)$$
$$Q_{AC} = \frac{3}{2}(V_d I_q - V_q I_d) \tag{6}$$

Assuming 100% efficiency, the instantaneous power at the DC side is

$$P_{DC} = P_{AC} \tag{7}$$

$$V_{DC} i_{DC} = \frac{3}{2} V_{td} I_d + \frac{3}{2} V_{tq} I_q \tag{8}$$

$$i_{DC} = \frac{3}{2}\frac{(V_{td} I_d + V_{tq} I_q)}{V_{DC}} \tag{9}$$

Therefore the dc-bus voltage dynamics can be written as

$$C\frac{dV_{DC}}{dt} = i_{in} - i_{RDC} - i_{DC} \tag{10}$$

where

$$\frac{dV_{DC}}{dt} = \frac{i_{in}}{C_{DC}} - \frac{V_{DC}}{R_{DC} C_{DC}} - \frac{3}{2}\frac{(V_{td} I_d + V_{tq} I_q)}{C_{DC} V_{DC}} \tag{11}$$

Multiplying both sides of (11) by $\boldsymbol{C_{DC} V_{DC}}$ have

$$\frac{d}{dt}\left(C_{DC}V_{DC}^2\right)=P_{in}-\frac{V_{DC}^2}{R_{DC}}-\frac{3}{2}\left(V_{td}I_d+V_{tq}I_q\right) \tag{12}$$

This can be rewritten as

$$\frac{d}{dt}\left(\frac{1}{2}C_{eq}V_{DC}^2\right)=P_{in}-\frac{V_{DC}^2}{R_{DC}}-\frac{3}{2}\left(V_{td}I_d+V_{tq}I_q\right) \tag{13}$$

Equation (13) which represents the instantaneous power balance between the dc-side and the ac-side is linear with respect to V_{DC}^2 but nonlinear with respect to I_d and I_d. The left side is the rate of energy variation of $C_{eq} = 2C_{DC}$. P_{in} is the incoming power from the RES through dc-link to the converter, V_{DC}^2 / R_{DC} is the power dissipation in R_{DC} . $\frac{3}{2}\left(V_{td}I_d + V_{tq}I_q\right)$ is the instantaneous power balance between the converter and the ac system.

Assuming the stored energy in the interface reactors is neglected, then $3/2\left(V_{td}I_d + V_{tq}I_q\right) = 3/2\left(V_{sd}I_d\right)$ [5-9] hence equation (13) reduces to

$$\frac{d}{dt}\left(\frac{1}{2}C_{eq}V_{DC}^2\right)=P_{in}-\frac{V_{DC}^2}{R_{DC}}-\frac{3}{2}V_{sd}I_d \tag{14}$$

4. Small Signal Development

Equation (14) can be re-arranged as

$$R_{DC}\frac{d}{dt}\left(\frac{1}{2}C_{eq}V_{DC}^2\right)+V_{DC}^2=R_{DC}P_{in}-\frac{3}{2}R_{DC}V_{sd}I_d \tag{15}$$

Linearizing (15) with respect to V_{DC} and representing the result in Laplace domain, we have

$$\widetilde{V}_{DC}(s)=\left\{\begin{array}{l}\dfrac{R_{DC}}{2V_{DCss}}\dfrac{1}{\left(\dfrac{R_{DC}C_{eq}}{2}s+1\right)}\widetilde{P}_{in}(s)\\ -\dfrac{3}{2}\dfrac{R_{DC}V_{sdss}}{2V_{DCss}}\dfrac{1}{\left(\dfrac{R_{DC}C_{eq}}{2}s+1\right)}\widetilde{I}_d(s)\\ -\dfrac{3}{2}\dfrac{R_{DC}I_{dss}}{2V_{DCss}}\dfrac{1}{\left(\dfrac{R_{DC}C_{eq}}{2}s+1\right)}\widetilde{V}_{sd}(s)\end{array}\right\} \tag{16}$$

where subscript “ss” and “~” represent the steady state and the small signal perturbations of a variable, respectively.

Also applying linearization method to equation (5) around their quiescent operating point, we have

$$\frac{d}{dt}\begin{bmatrix}\widetilde{I}_d\\ \widetilde{I}_q\end{bmatrix}=\begin{bmatrix}-R/L & \omega & 0\\ -\omega & -R/L & 0\end{bmatrix}\begin{bmatrix}\widetilde{I}_d\\ \widetilde{I}_q\end{bmatrix}+\begin{bmatrix}-1/L & 0\\ 0 & -1/L\end{bmatrix}\begin{bmatrix}\widetilde{V}_{td}\\ \widetilde{V}_{tq}\end{bmatrix}+\begin{bmatrix}-1/L & 0\\ 0 & 0\end{bmatrix}\begin{bmatrix}\widetilde{V}_{sd}\\ 0\end{bmatrix} \tag{17}$$

5. The Equivalent Circuit

The equations of the state-space representation (equation 17) can be written as

$$\widetilde{V}_{td}-\widetilde{V}_{sd}=L\frac{d\widetilde{i}_d}{dt}+R\widetilde{i}_d-\omega L\widetilde{i}_q \tag{18}$$

$$\widetilde{V}_{tq}=L\frac{d\widetilde{i}_q}{dt}+R\widetilde{i}_q+\omega L\widetilde{i}_d \tag{19}$$

From the two equations the following equivalent circuit is derived:

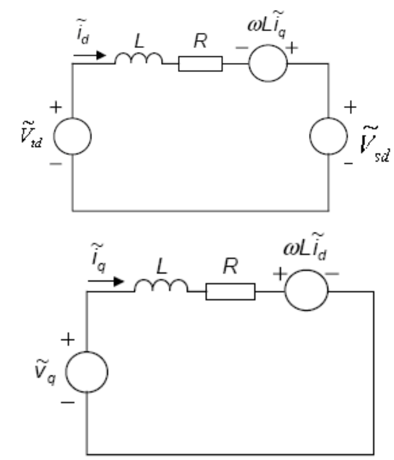

Figure 2. Equivalent Small signal circuit for AC side in dq coordinates

6. Design Process of the Controllers

Controlling the time invariant quantities is simple and can be achieved using PI, PD, or PID controller. In the following control scheme a cascaded control structure is used, i.e. the output of one controller is used as the reference of the other. Hence the controllers become main criteria in designing the control parameters.

6.1 DC Side

The DC-link voltage V_{DC} is controlled by a PI regulator; the actual dc voltage is compared with the reference dc voltage V_{dc}^*. The error signal is passed through the PI controller to provide reference current I^* for the current controller.

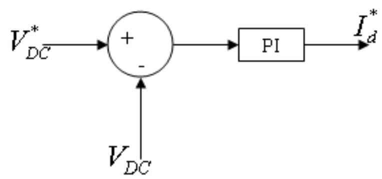

Figure 3. The dc-bus controller

6.2 AC side Decoupled Current control

The small-signal model of the ac-side of the converter (equation 18 and 19) can be used for the design of the current controllers, which is based on proportional and integral (PI) actuations. Poles and zero of the compensators should be located with the objective of achieving good static and dynamic performance of the system, and providing sufficient margins.

To decouple the d and q current components in 17, the following changes of variable are defined [9], [10]

$$\tilde{V}_{td} = \Delta\tilde{V}_d - \omega L\tilde{i}_q + \tilde{V}_{sd}$$
$$\tilde{V}_{tq} = \Delta\tilde{V}_q + \omega L\tilde{i}_d \tag{20}$$

in which

$$\Delta\tilde{V}_d = L\frac{d\tilde{i}_d}{dt} + R\tilde{i}_d \quad and \quad \Delta\tilde{V}_q = L\frac{di_q}{dt} + R\tilde{i}_q \tag{21}$$

$$\frac{d\tilde{i}_d}{dt} = -\frac{R\tilde{i}_d}{L} + \frac{1}{L}\Delta\tilde{V}_d$$
$$\frac{d\tilde{i}_q}{dt} = \frac{-R\tilde{i}_q}{L} + \frac{\Delta\tilde{V}_q}{L} \tag{22}$$

Equation 22 represents two first-order, decoupled subsystems with $\Delta\tilde{V}_d$ and $\Delta\tilde{V}_q$ being the new control variables which can be deduced from the two independent controllers PI controllers. $\tilde{V}_{sd}$ is a feed-forward term to speed up the control response to the ac line voltage disturbance.

From these equations the control diagram is obtained thus:

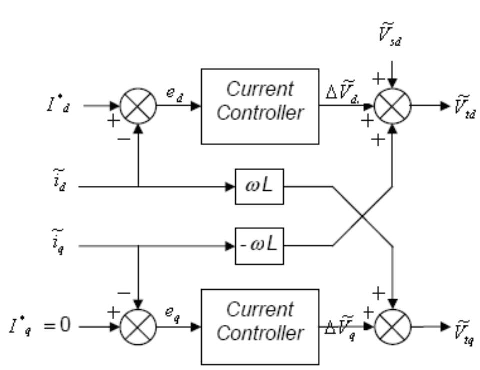

Figure 4. The decoupled current controller block diagram

If a PI controller is defined by

$$\Delta\tilde{V}_d = K_p e_d + K_i\int_0^t e_d\,dt \tag{23}$$

The transfer function, of the controller

$$\frac{\Delta\tilde{V}_d(s)}{e_d(s)} = G_c(s) = K_p + \frac{K_i}{s} = \frac{K_p}{s}\left(s + \frac{K_i}{K_p}\right)$$

where

$$e_d = I^* - i_d \tag{24}$$

The open-loop gain in the frequency domain is

$$G_o(s) = \frac{K_p}{s}\left(s + \frac{K_i}{K_p}\right)\frac{1}{Ls + R} \tag{25}$$

Choosing $K_p = L/\tau_i$ and $K_p = R/\tau_i$, the open-loop and close-loop system respectively becomes

$$G_o(s) = \frac{1}{\tau_i s} \tag{26}$$

$$G_c(s) = \frac{I_d(s)}{I^*_{dc}(s)} = \frac{1}{\tau_i s + 1} \tag{27}$$

where τ is the time constant which determines the current controller response time and is usually chosen in the range of 1.5ms to 5ms.

Similarly, the quadrature current controller is designed in the same way. Hence,

$$G_c(s) = \frac{I_q(s)}{I_{qref}(s)} = \frac{1}{\tau_i s + 1} \tag{28}$$

The active and reactive power are proportional to i_d and i_q respectively. The q-axis current determines the displacement factor on the grid side of the inductors. To operate the converter with unity power factor implies a zero reference q-current $\left(I_q^* = 0\right)$.

6.3 Providing control references to the modulator

Defining $\tilde{V}_{td}$ and $\tilde{V}_{tq}$ with respect to the amplitude m_k and phase ϕ of the modulating waveform with no positive offset it added to it [9],

$$V_{td} = \frac{m}{2}\left[V_{C1} + V_{C2}\right]Cos\,\phi \tag{29}$$

$$V_{tq} = \frac{m}{2}\left[V_{C1} + V_{C2}\right]Sin\,\phi \tag{30}$$

Assuming

$$V_{C1} = V_{C2} = \frac{V_{DC}}{2}$$

$$V_{td} = \frac{m}{2} V_{DC} Cos\phi$$

$$V_{tq} = \frac{m}{2} V_{DC} Sin\phi$$

then

$$\phi = \tan^{-1}\left(\frac{V_{tq}}{V_{td}}\right)$$

$$m = \frac{2\sqrt{V_{td}^{2} + V_{tq}^{2}}}{V_{DC}} \qquad (31)$$

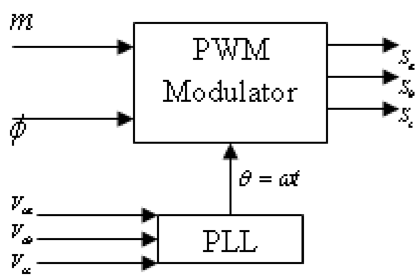

Figure 5. Block diagram of the modulator and the phase locked-loop (PLL)

6.4 The modulator

The above state-space model assumes that the control variables of the converter are V_d and V_q instead of the duty cycles of the switches. The controller based on this model provides control references to the modulator, which is responsible for generating the voltages in the converter. Although this method avoids using duty cycles in the model, accurate measure of the DC-link voltage will be required not only for the controller, but also for the modulator.

7. Simulation Results

A MATLAB simulink of the model was developed, the RES and its converter is modeled as a current source that provides $i_{in} = P_{in} / V_{DC}$ into the NPC converter connected to the grid. Selected perturbations and system response waveforms from the simulation are illustrated in Figs. 6 - 8.

7.1 Reactive power change

Initially, real power flows of 0.05MW from RES to the grid with Vdcref set to 500V, at t= 0.6s, Iqref is changed from 0 to -0.2KVA. Fig. 6 shows the dynamic response of the system. Fig. 6(a) shows the variation of the modulation index of the system to meet the power flow requirements.

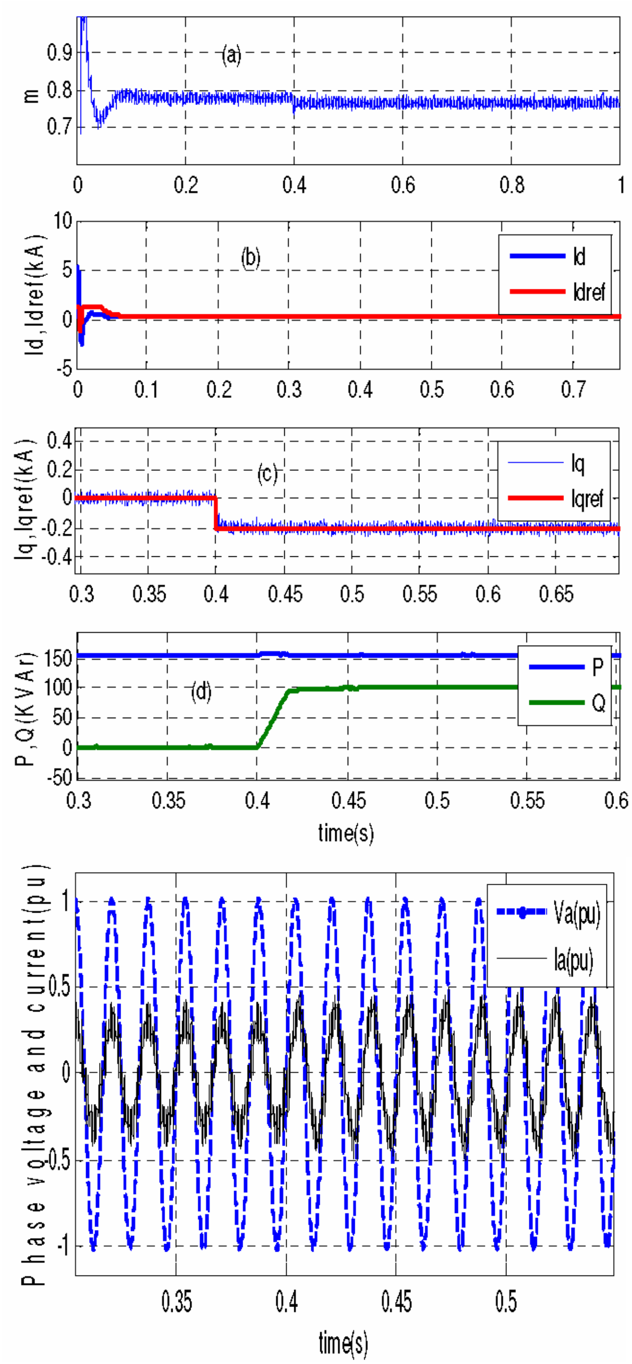

Figure 6. System response to a step change in 1qref from 0 to -0.2KA

7.2 Step Change in V_{DCref}

Initially, 5kW P_{in} power flows from the dc side to the ac side. At time = 0.6s, V_{DCref} is changed from 500V to 600V and the response of the system is shown in fig. 7.

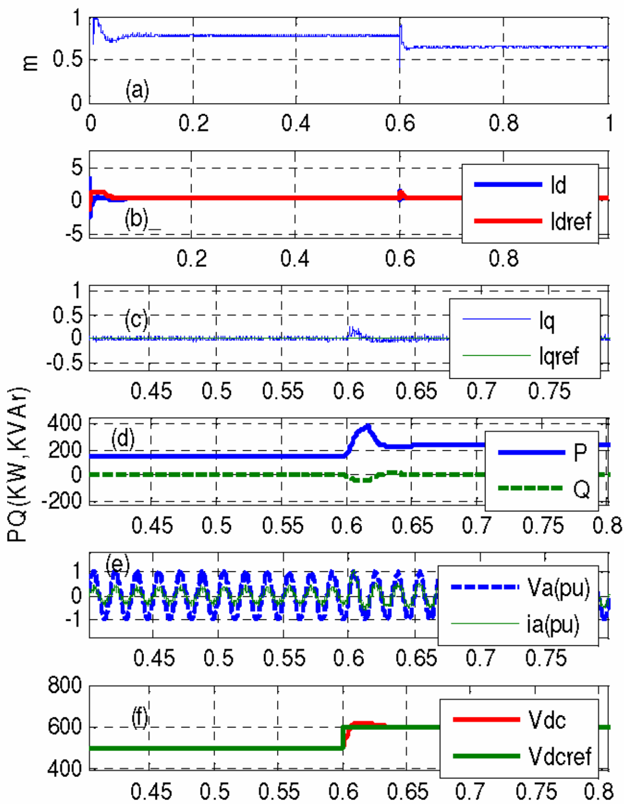

Figure 7. System response to a step change in Vdcref from 500V to 600V

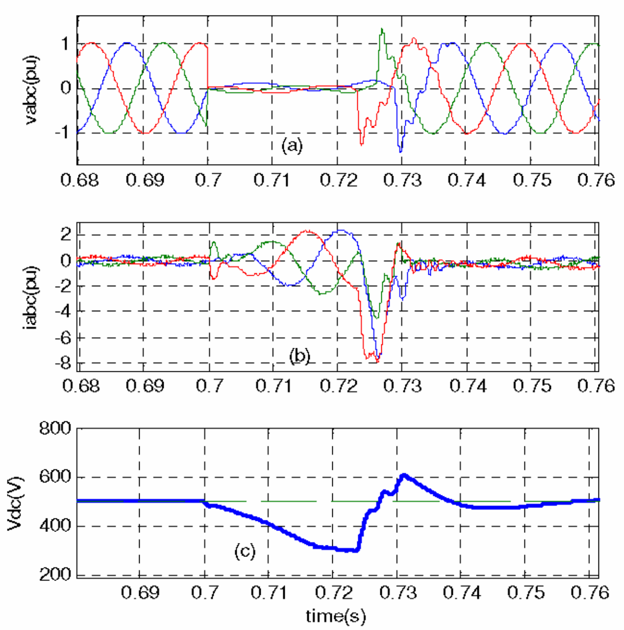

Figure 8. System response to a three-phase to ground fault for a period of 20ms. (a) The three-phase voltage Vsabc (pu) (b). Three-phase current iabc (pu) .(c) The Vdc

7.3 Three-phase fault

The entire system is under steady-state condition with Vdc= 500V and Pin = 0.05MW. At t=0.7s, the grid is subjected to a three-phase to ground fault for 20ms. Fig.8 shows the system response to this disturbance

8. Conclusion

Dynamic model of a system comprising grid connected renewable energy system (RES) via a three-level neutral Point Diode Clamped converter (NPC) is presented. The analysis and control scheme which is done in a dq reference frame is intended to achieve constant dc-link, obtain unity power factor and allow bi-directional power flow.

Exploration of the dynamic response of the entire system under certain perturbations on the AC side and DC-bus are studied and presented.

References

[1] M. H. RASHID Power Electronics handbook Academic Press Series in Engineering, Auburn University, Series Editor

[2] A. F Nnachi, A.A Jimoh, and D.V Nicolae, Multilevel High Power Converters for Reversible Power Flow between Utilities and Power Pool Transmission Corridor. IEEE Africon 2007 26 - 28 September 2007 Windhoek Country Club and Resort, Windhoek, Namibia 2007.

[3] A. Yazdani, R. Iravani, An Accurate Model for the DC-Side Voltage Control of the Neutral Point Diode Clamped Converter, IEEE trans. on power delivery, vol. 21, no. 1, January 2006.

[4] D. G. Holmes, T. A. Lipo, Pulse Width Modulation for Power Converters Principles and Practice (IEEE press-Willy Interscience. 2003)

[5] R. Pena, R. Cardenas, R. Blasco, G. Asher, and J. Clare, A cage induction generator using back to back PWM converters for variable speed grid connected wind energy system, in proc. IEEE Industrial Electronics Conf., vol. 2, 2001, pp. 1376 – 1381.

[6] Y. Ye, M. Kazerani, and V. H. Quintana, Modeling, control, and implementation of three-phase PWM converters, IEEE Trans. Power Electronics, vol.18, no. 3, pp. 857 – 864, May 2003.

[7] A. Yazdani, R. Iravani, An Accurate Model for the DC-Side Voltage Control of the Neutral Point Diode Clamped Converter, IEEE trans. on power delivery, vol. 21, no. 1, January 2006.

[8] C. K. Sao, P. W. Lehn, M. R. Iravani, and J. A. Martinez, A benchmark system for digital time-domain simulation of a pulse-width-modulated D-STATCOM, IEEE Trans. Power Del., vol. 17, no.4, pp. 1113 – 1120, Oct. 2002.

[9] A. Yazdani and R. Iravani, Dynamic Model and Control of the NPC-Based Back-to-Back HVDC System. IEEE Transaction on Power Delivery, Vol. 21. No.1 January 2006

[10] C. Schauder and H. Mehta, Vector analysis and control of advanced static VAR compensators, Proc. Inst. Elect.Eng.-C, vol. 140, pp. 299 – 306, July. 1993

[11] R. Uhrin, F. Profumo, Stand-alone AC/DC Converter for Multiple Inverter Applications IEEE 1996, pp. 120 – 126.